

Contents

1. Upcoming Release of AFDEX_V26R01

2. AFDEX Analysis Case Studies

- 2.1 Anisotropic Forming Analysis of Auto Parts
- 2.2 Double Row Progressive Process Analysis
- 2.3 Remeshing Improvements for Severe Self-Contact Problem
- 2.4 Identifying Lubrication Regime Change
- 2.5 Finite Element Analysis on Dynamic and Static Recrystallization and Grain Growth of SCM440

3. Major UI Improvements

- 3.1 STEP/IGES Import Support for 3D Models
- 3.2 Addition of Hill 1948 Anisotropic Model

4. News & Announcements

- 4.1 On-site Seminars & Consulting

1. Upcoming Release of AFDEX_V26R01

The release of AFDEX_V26R01 is scheduled for June 2026. We are currently preparing for this launch, which will incorporate the new features and enhancements introduced in the Q1 newsletter as well as this current issue.

2. AFDEX Simulation Case Studies

2.1 Anisotropic Forming Analysis of Auto Parts

To evaluate the applicability of the newly developed anisotropic finite element analysis (FEA) program, the forming process of a strut mount main plate was simulated using this anisotropic model.

Figure 2.1 compares the conventional isotropic finite element result and the anisotropic finite element analysis result with the experimental outcomes. For sheet metal forming using solid elements, by applying a perspective view to both the isotropic and anisotropic analysis results, a more accurate comparison with the experimental results was achieved.

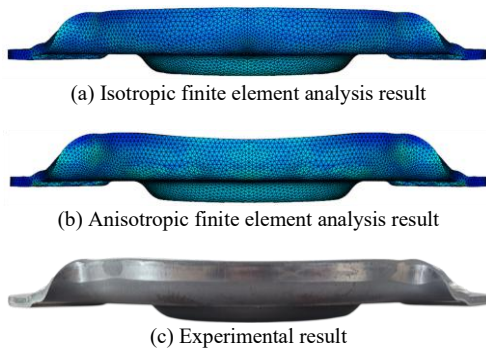


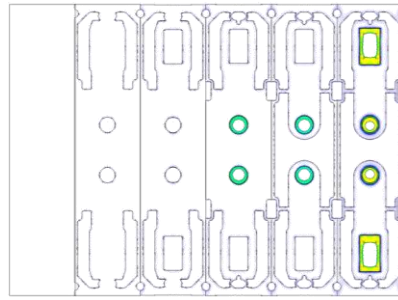
Figure 2.1 Comparison of analysis and experimental results for the strut mount main plate

As a result, while the isotropic FEA predicted a flat top surface, the anisotropic analysis accurately predicted a concave, depressed shape, which aligns closely with the experimental results.

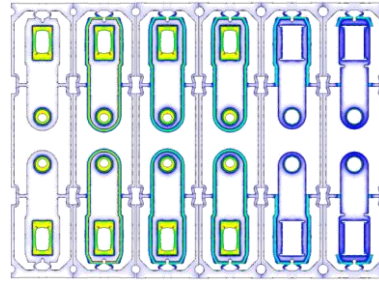
2.2 Double Row Progressive Process Analysis

The progressive process is a standard mass-production method that performs multi-stage forming while continuously feeding strip material. The material used for the negative current collector component of a lithium-ion battery is a C1100 copper sheet with a thickness of 1.5 mm. Excluding idling stations, this process consists of a total of 17 stages, combining blanking, piercing, forming, and bending operations.

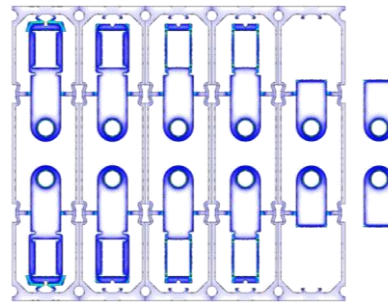
The forming analysis was conducted based on a 90-degree symmetric model utilizing the sheet metal forging elastoplastic module. The stage-by-stage forming analysis results can be seen in Figure 2.2.



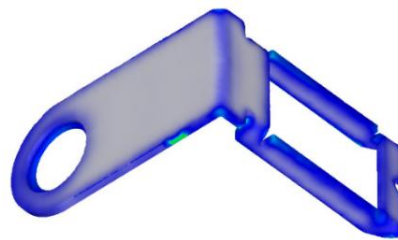
(a) Input material and deformation history from stages 1 to 5



(b) Deformation history from stages 6 to 11



(c) Deformation history from stages 12 to 17

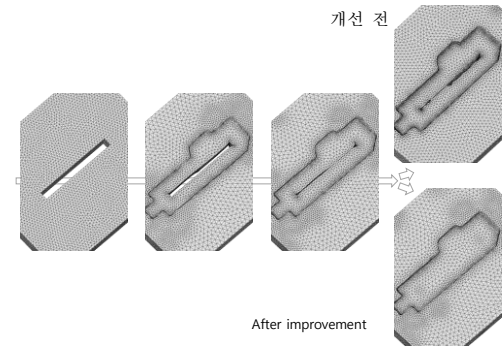


(d) Predicted geometry of the current collector component

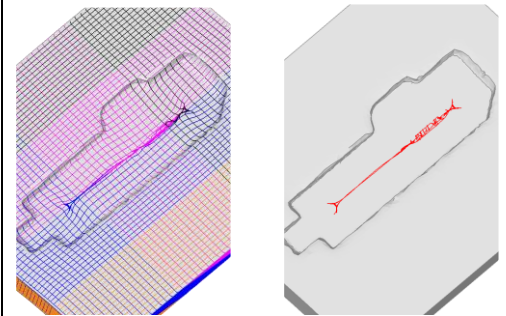
Figure 2.2 Double-row progressive process analysis of the current collector component

2.3 Remeshing Improvements for Severe Self-Contact Problem

As shown in Figure 2.3, using a preform with internal holes to reduce input material weight and forming loads can sometimes lead to material-to-material self-contact. In such cases, problems may occur in the regions where materials contact each other during the remeshing process, causing the simulation to stop. If material penetration occurs, remeshing becomes inevitable, which can lead to volume loss. The program has been improved so that even when self-contact occurs, the materials are successfully merged into a single entity through remeshing, as seen in the "After Improvement" section of Figure 2.3(a). In real-world scenarios, material bonding occurs under high-temperature and high-pressure environments; even if we assume that welding essentially takes place, it does not affect the macroscopic results. Furthermore, the bonded surface (i.e., the welded surface) can still be identified through the metal flow lines in Figure 2.3(b) or the folding information in Figure 2.3(c).



(a) Deformation history

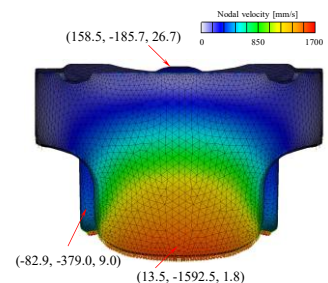


(b) Metal Flow lines (c) Folding
Figure 2.3 Example of Self-Contact

2.4 Identifying Lubrication Regime Change

From a macroscopic perspective, bulk metal forming processes, particularly forging can be viewed as a battle between flow characteristics supported by an entire material and friction exerting local influence at the interface. Empirically, in the forging of steel, the flow characteristics supported by strain hardening dominate the metal forming deformation of the material. Recently, with the increasing trend of forging non-ferrous metals like aluminum, which have significantly lower strain hardenability compared to that of steel, forging CAE application engineers will find their confidence in simulation accuracy—built upon years of steel forging—challenged. This confusion arises as the flow characteristics and the friction begin to share dominance. Following the publication of the paper on Lubrication Regime Change (LRC) [S. W. Lee, J. M. Lee, M. S. Joun, 2020, On critical surface strain during hot forging of lubricated aluminum alloy, Tri. Int. 141 105855] in 2020, the AFDEX development group has conducted extensive research on this topic.

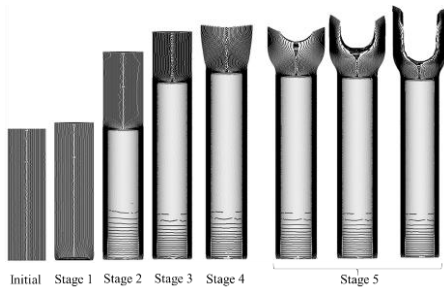
Figure 2.4 shows examples where LRC occurred. Analysis results obtained without considering LRC—meaning relying on conventional friction laws—show distinct discrepancies from experimental results in critical engineering areas. In the case of Figure 2.4(a), if LRC is not considered, the bottom center area becomes concave, which contradicts the convex shape observed in the experiment. In Figure 2.4(b), while a 0.2 mm misalignment between the punch and the lower die caused a real-world earing height difference of 2.2 mm at the top of the forged product, the conventional friction law without LRC predicted a value of less than 0.6 mm. However, when LRC was considered, an earing height difference of 2.04 mm was accurately predicted.



Before improvement

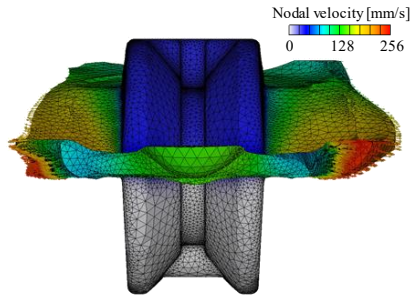


(a) Hot forging of A4032 alloy piston (Nodal velocity distribution)

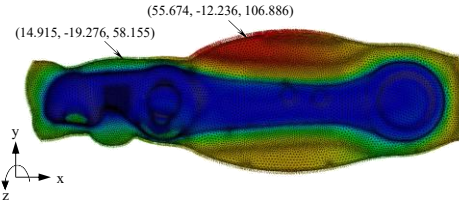


(b) Automatic multi-stage cold forging of A6082-T6 alloy yoke
Figure 2.4 Cases of LRC occurrence

Figure 2.5 shows processes where deformation shapes can be accurately predicted from an engineering perspective without needing to consider the possibility of LRC. Figure 2.5(a) displays the analysis results of the hot forging process for an S45C construction machinery part. This process achieved satisfactory results using a conventional friction law with a friction coefficient of 0.3 [M. K. Razali, S. W. Kim, M. Irani, M. C. Kim, M. S. Joun, 2021, *Practical quantification of the effects of flow stress, friction, microstructural properties, and the tribological environment on macro- and micro-structure formation during hot forging*, Tri. Int., V. 164, 107226]. Figure 2.5(b) shows the analysis results of the hot forging process for an A6082 alloy lateral arm. When a conventional friction law with a friction coefficient of 0.15 was applied, the analysis results aligned with the experimental results from an engineering standpoint [J. H. Park, S. M. Ji, J. M. Choi, M. S. Joun, *Accurate flow characterization of A6082 for precision simulation of a hot metal forming process*, Materials, 15, 8656].



(a) Hot forging of S45C construction machinery part (Nodal velocity distribution)



(b) Hot forging of A6082 alloy lateral arm (Nodal velocity distribution)

Figure 2.5 Cases where the influence of LRC is negligible

Comparing Figures 2.4 and 2.5, LRC is highly likely to occur when the material flow aligns with the forging direction (the direction of punch movement), such as in forward or combined forward-backward extrusion. Conversely, when the material flow is in a lateral direction, LRC does not occur, and conventional friction laws can be safely used without engineering issues.

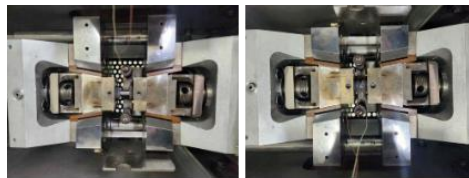
According to various studies by the development group, the likelihood of LRC increases as the material's strain hardening decreases, the effective strain at the interface increases, and the lubrication conditions worsen. Therefore, the probability of LRC occurring in the cold

and hot forging of aluminum is significantly higher than that of steel. When LRC occurs, localized interfacial characteristics significantly influence the overall material flow, complicating the forging process. Thus, this high probability of LRC, combined with a narrow hot forging temperature range, is a major factor that makes aluminum forging challenging.

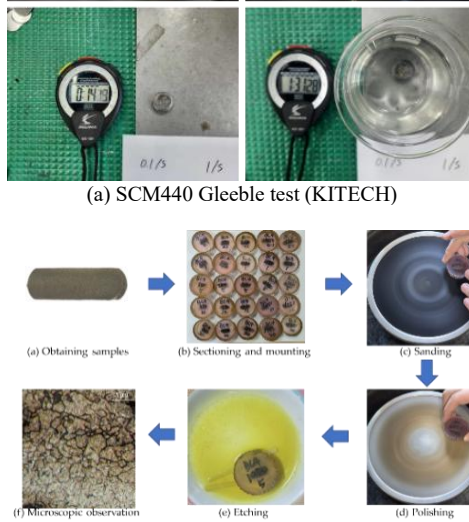
When LRC occurs, utilizing a generalized Coulomb friction law with a variable friction coefficient that accounts for LRC is essential for precise forging simulation, particularly for accurately predicting localized shapes.

2.5 Finite Element Analysis of Dynamic and Static Recrystallization and Grain Growth of SCM440

The MFRC-Gyeongsang National University research team, led by Dr. Razali, investigated the dynamic recrystallization (DRX), static recrystallization (SRX), and grain growth (GG) phenomena occurring during the hot compression of SCM440 steel through a combination of experiments and simulations. Compression tests were conducted over a temperature range of 850~1250°C and a strain rate range of 0.1~20 s⁻¹ to analyze microstructural changes under various conditions. By measuring grain sizes, the transition process from DRX to SRX and GG was tracked. Using an optimization technique that integrates AFDEX and Siemens/Altair HyperStudy, key kinetic parameters were derived, and the correlation between the FEA simulation results and experimental data was analyzed. The results are summarized in Figure 2.6.

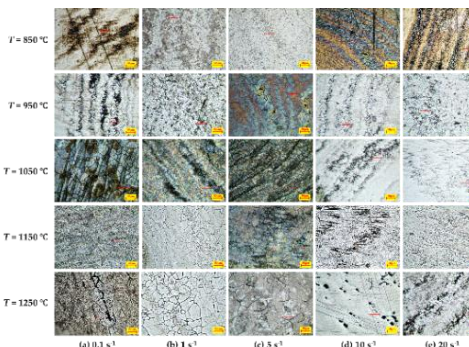


(a) SCM440 Gleeble test (KITECH)

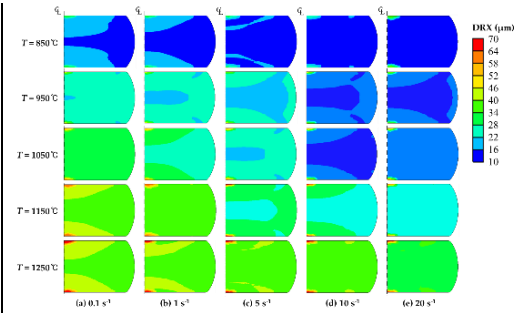


(b) Metallographic specimen preparation process

The developed integrated model accurately predicts grain size changes during the deformation and post-deformation stages, showing excellent agreement with experimental results. This study provides an effective tool for understanding and optimizing the hot forming processes of alloy steels.



(c) Optical micrograph of DRX microstructure



(d) FEM prediction of $d_{DRX,avg}$

Figure 2.6 Microstructure experiment and analysis

3. Major UI Improvements

3.1 STEP/IGES Import Support for 3D Models

To improve the versatility of 3D modeling data, support for importing STEP and IGES files will be newly added starting from AFDEX V26R01. This allows original CAD data to be used directly in simulations without a separate file conversion process, thereby minimizing data loss and significantly improving workflow efficiency.

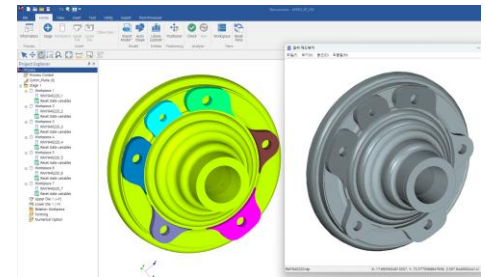


Figure 3.1 STP file loading screen

3.2 Addition of Hill 1948 Anisotropic Model

The Hill 1948, one of the well-known anisotropic yield criteria has been added to further elevate the precision of forming simulation. It is now possible to more intricately reflect the mechanical properties of materials which vary according to the rolling direction in the simulation. As shown in Figure 3.2, users can directly input the anisotropic coefficients F, G, H, L, M, and N, or utilize two supported methods for inputting R-values.

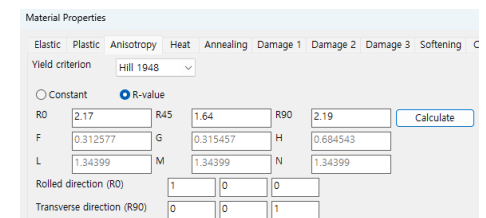


Figure 3.2 Anisotropic coefficient input dialog

4. News & Announcements

4.1 On-site Seminars & Consulting

Since the beginning of this year, we have been actively conducting on-site visits, on-site seminars, consulting, and feedback-gathering sessions with our users. In the first quarter alone, these activities have already been carried out with 11 domestic companies and 3 overseas companies. When a user company or a potential client requests a seminar topic, we prepare customized materials and deliver the seminar accordingly.



Figure 4.2 Technical seminar on flow characteristics and friction at Jinhap Co., Ltd